

## Exact Action Spectra for Cellular Responses Relevant to Phototherapy

T.I. KARU, Ph.D.,<sup>1</sup> and S.F. KOLYAKOV, M.S.<sup>2</sup>

### ABSTRACT

**Objective:** The aim of the present work is to analyze available action spectra for various biological responses of HeLa cells irradiated with monochromatic light of 580–860 nm. **Background data:** Phototherapy (low-level laser therapy or photobiomodulation) is characterized by its ability to induce photobiological processes in cells. Exact action spectra are needed for determination of photoacceptors as well as for further investigations into cellular mechanisms of phototherapy. **Methods:** Seven action spectra for the stimulation of DNA and RNA synthesis rate and cell adhesion to glass matrix are analyzed by curve fitting, followed by deconvolution with Lorentzian fitting. Exact parameters of peak positions and bandwidths are presented. **Results:** The peak positions are between 613.5 and 623.5 nm (in one spectrum, at 606 nm), in the red maximum. The far-red maximum has exact peak positions between 667.5 and 683.7 nm in different spectra. Two near infrared maxima have peak positions in the range 750.7–772.3 nm and 812.5–846.0 nm, respectively. **Conclusions:** In the wavelength range important for phototherapy (600–860 nm), there are four “active” regions, but peak positions are not exactly the same for all spectra.

### INTRODUCTION

**A**N ACTION SPECTRUM is a plot of the relative effectiveness of different wavelengths of light in causing a particular biological response, and under ideal conditions, it should mimic the absorption spectrum of the molecule that is absorbing the light and whose photochemical alteration causes the effect.<sup>1,2</sup> The first action spectra, with the aim to prove or disprove the existence of so-called laser biostimulation effect on cellular level, were recorded in the early 1980s.<sup>3–5</sup> Laser biostimulation (nowadays called low-level laser therapy, low-power laser therapy, photobiomodulation, or phototherapy) as a medical treatment goes back to the 1960s with the use of a He-Ne laser (which was the first commercially available laser) for the improvement of healing of impaired wounds. The reasons why this method was, for a long time, held in suspicion and why it is still outside mainstream medicine are analyzed elsewhere.<sup>1,6</sup> The action spectra in the visible-to-near infrared (IR) region measured for biological responses of cultured cells showed that red light at 632.8 nm was not the only wavelength suitable for laser biostimulation.<sup>3–5</sup> These spectra, together with the results of experiments of dichromatic irradiation of cells and modifi-

cation of light effects with chemicals,<sup>7,8</sup> showed that “laser biostimulation” is a photobiological phenomenon. These data also suggested that the photoacceptor for stimulation of cell metabolism is the terminal enzyme of the respiratory chain (i.e., cytochrome c oxidase for eukaryotic cells<sup>9</sup> and the cytochrome bd complex for *Escherichia coli*<sup>10</sup>). In the blue spectral region, flavoproteins such as NADH-dehydrogenase can work as photoacceptors.<sup>8</sup> The suggestion that cytochrome c oxidase is a photoacceptor molecule has been recently confirmed in elegant experiments with functionally inactivated primary neurons, proposing that light upregulates this enzyme.<sup>11</sup>

To make suggestions about photoacceptors inside the cytochrome c oxidase molecule, action spectra recorded for the stimulation of DNA and RNA synthesis rate<sup>4,5</sup> as well as that for the increase of cell adhesion<sup>12</sup> were summarized and called the “action spectrum of proliferation increase.”<sup>9</sup> With the advent of sophisticated computer software for analyzing recorded spectra, action spectra can now be analyzed with much greater accuracy. This is the goal of the present work.

Two recent publications<sup>1,11</sup> encouraged us to perform the present work. In this work, we analyzed individual action spectra of various biological responses of HeLa cells recorded

<sup>1</sup>Institute of Laser and Information Technologies and <sup>2</sup>Institute of Spectroscopy, Russian Academy of Sciences, Troitsk, Moscow Region, Russian Federation.

earlier<sup>4,5,12</sup> in the wavelength range of 580–860 nm, with the goal of obtaining exact data for peak positions and bandwidths. These data might help to define the primary photoacceptor (probably one of the intermediates of cytochrome c oxidase appearing during turnover<sup>9</sup>) and to find the optimal wavelengths for phototherapy. Finally, we hope that this work will encourage others to record new action spectra to clear cellular mechanisms of phototherapy.

It should be noted that HeLa cells were used as a well-known model system (a radiobiological standard). The measured action spectra are thought to coincide with the respective spectra recorded on other cells cultured *in vitro*, due to the similarity of respiratory chains and cytochrome c oxidase, in particular. We also hope that this work will encourage measurements of clinical action spectra, which are still absent. However, clinical action spectra may differ from the spectra measured on cell monolayers due to light scattering and nonhomogeneity of multilayer tissues.

## MATERIALS AND METHODS

### Cells

HeLa cells, obtained from the Institute of Virology, Moscow, Russia, were cultivated as a monolayer in closed scintillation vials (diameter 24 mm) at 72 h (to mid-logarithmic phase of growth) or 240 h (plateau-phase of growth) at 37°C in 2 mL of nutrient medium 199, which contained 10% bovine serum and 100 U/mL of streptomycin and penicillin.<sup>3,13</sup> Figure 1 presents the growth curve (the change in cell number with time) after seeding  $1 \times 10^5$  HeLa cells per scintillation vial. The arrows indicate the points when the irradiation experiments were performed. The number of cells per vial was  $2.5\text{--}6 (\pm 0.2) \times 10^5$  cells (the model of log-phase culture) or  $1.0 (\pm 0.3) \times 10^6$  cells (the model of plateau-phase culture). The labeling index ( $I_s$ ) of the log-phase population was  $19.1 (\pm 3.0)\%$  and that of the

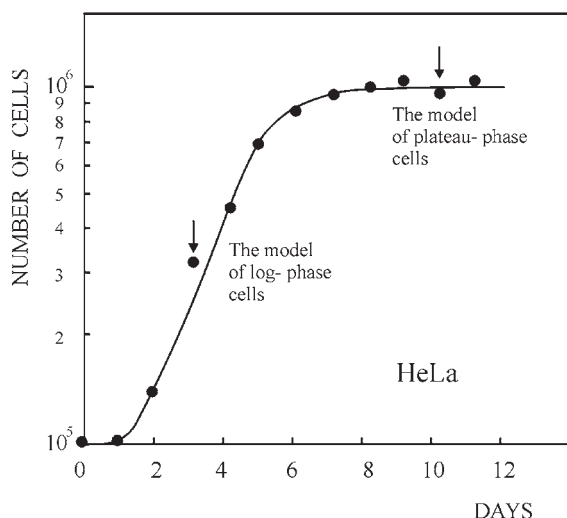


**FIG. 1.** The growth curve of HeLa cells in a scintillation vial.<sup>13</sup>

plateau-phase culture  $5.0 (\pm 0.8)\%$ . The mitotic indices ( $I_m$ ) of the log-phase and plateau-phase populations were  $1.1 (\pm 0.1)\%$  and  $0.1\%$ , respectively.<sup>13</sup> One should note that, using this type of cell cultivation in closed vials, some limitations of oxygen availability occur, especially in the case of the plateau phase cultures.

### Irradiation

Cells were irradiated through the bottom of the scintillation vial covered with the monolayer. During the irradiation, the vial was in an inclined position (i.e., the monolayer was not covered by the nutrient medium), as shown in Figure 2A. Using this experimental scheme, we did not disturb the environment (oxygen partial pressure, pH, temperature) or sterile conditions inside the vial. For the action spectrum of cell adhesion, a suspension was prepared from the log-phase population and irradiated as a thin layer in a laboratory-made glass vial (Fig. 2B). The number of the cells in the vial (130  $\mu$ L) was 85,000, and the suspension exactly filled the cuvette. The optimal irradiation conditions (shape and the dimensions of the vial, number of cells per vial) were developed in a special series of the experiment.<sup>12</sup> The irradiation schemes are summarized elsewhere.<sup>14</sup> The Spectra Physics M404 power meter was used for the measurement of light intensity.

Handling of the cells and irradiation were performed in the dark or in dim natural light.

### Recording of action spectra

Descriptions of measurements of DNA and RNA synthesis rate with radioactive precursors  $H^3$ -thymidine and  $C^{14}$ -uridine as well as measurement of cell adhesion can be found, respectively, in Karu et al.<sup>3</sup> and Karu et al.<sup>12</sup> DNA and RNA synthesis rates were measured at 1.5 or 4.0 h after the irradiation in log-phase and plateau-phase cultures, respectively. Cell adhesion to glass matrix was measured 30 min after the irradiation. Light sources and types of wavelength filtration are described below, together with the analysis of every spectrum.

### Statistical analysis

Experimental data are expressed in terms of the mean  $\pm$  SEM from 10 measurements. These data were digitized and used for curve fitting and deconvolution of the spectra using Lorentzian fitting with the software program Origin 7.5 (OriginLabs Corp., Northampton, MA).

## RESULTS AND DISCUSSION

Figure 3 presents five action spectra in the red-to-near IR region, and Table 1 provides the data of their deconvolution. Original experimental data<sup>4,5,12</sup> are presented here, together with curve fitting and Lorentzian fitting. Mean-square deviation  $R^2$  for every fitting is also shown in Table 1. At the best fitting,  $R^2 = 1$ . Spectra A and B present stimulation of DNA synthesis rate in log-phase and plateau-phase cultures, respectively. Spectra C and D are the dependencies of stimulation of RNA synthesis rate in log- and plateau-phase cells. These four spectra were re-

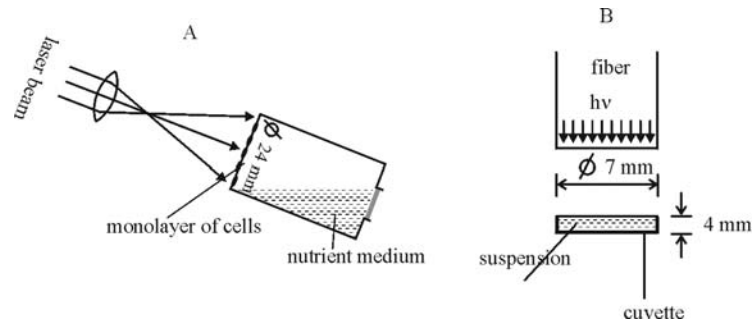


FIG. 2. Irradiation schemes of a cell monolayer grown in the closed scintillation vial (A) and a cell suspension prepared from a cell monolayer (B).

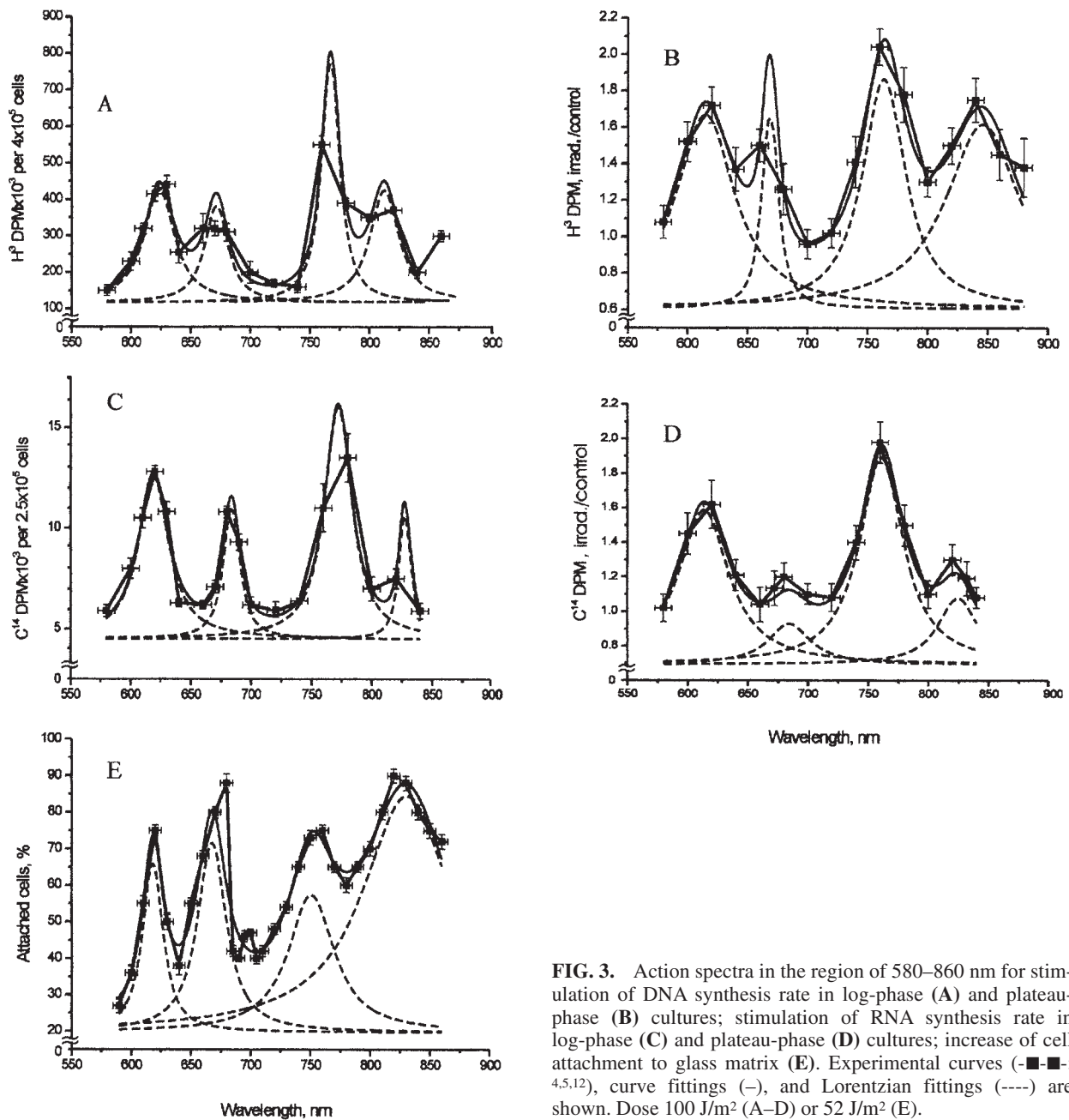


FIG. 3. Action spectra in the region of 580–860 nm for stimulation of DNA synthesis rate in log-phase (A) and plateau-phase (B) cultures; stimulation of RNA synthesis rate in log-phase (C) and plateau-phase (D) cultures; increase of cell attachment to glass matrix (E). Experimental curves (—■—■—; 4.5,12), curve fittings (—), and Lorentzian fittings (----) are shown. Dose 100 J/m<sup>2</sup> (A–D) or 52 J/m<sup>2</sup> (E).

TABLE 1. PARAMETERS OF THE BANDS IN ACTION SPECTRA IN FIGURE 3 DETERMINED BY DECONVOLUTION OF SPECTRA WITH LORENTZIAN FITTING

Stimulation of DNA synthesis rate				Stimulation of RNA synthesis rate				Increase of cell adhesion to glass matrix	
Proliferating culture Fig. 3A ( $R^2 = 0.97$ )		Plateau-phase culture Fig. 3B ( $R^2 = 0.98$ )		Proliferating culture Fig. 3C ( $R^2 = 0.98$ )		Plateau-phase culture Fig. 3D ( $R^2 = 0.93$ )		Proliferating culture Fig. 3E ( $R^2 = 0.91$ )	
Peak position, nm	FWHM, nm	Peak position, nm	FWHM, nm	Peak position, nm	FWHM, nm	Peak position, nm	FWHM, nm	Peak position, nm	FWHM, nm
623.5	29.5	615.0	58.1	619.1	29.0	613.5	49.4	618.0	18.9
671.5	22.1	668.7	13.8	683.7	14.7	684.5	41.6	667.5	27.8
767.3	16.4	763.7	42.1	772.3	26.0	761.1	43.3	750.7	45.6
812.5	28.1	—	—	—	—	—	—	—	—
—	—	—	—	827.5	9.5	824.7	39.1	830.7	89.3
—	—	846.0	74.5	—	—	—	—	—	—

$R^2$ , mean-square deviation; FWHM, full width of the band at half maximal height.

corded using monochromator MDR-2 (LOMO, St. Petersburg, Russia) with a halogen lamp with the power of 150 W placed in a parabolic reflector. Spectral full width at half maximum (FWHM) of the produced light was 14 nm (shown also in Fig. 3A–D). Light intensity was kept constant (10 W/m<sup>2</sup>) by varying the voltage across the halogen lamp. Irradiation time was 10 sec, and dose was 100 J/m<sup>2</sup>. Spectrum E shows an increase of cell attachment to a glass matrix. In this case, the monochromator was a more advanced one constructed in Institute of Spectroscopy of Russian Academy of Science.<sup>12</sup> Light parameters for recording of this spectrum were as follows: I = 1.3 W/m<sup>2</sup>, t = 40 sec, D = 52 J/m<sup>2</sup>, FWHM 10 nm.

All five spectra in Figure 3 are characterized by four wide maxima, but the exact peak positions are different (Table 1). The largest differences in peak position can be seen in the near IR region above 800 nm. This peak appears at 812.5 nm in the spectrum A, between 827.5 and 830.7 nm in the spectra C, D, and E, and at 846.0 nm, in the spectrum B. The oxidized form of cytochrome c oxidase has a broad absorption band above 800 nm that is centered at 830 nm.<sup>15</sup> Cu<sub>A</sub>, a dimeric copper complex with four ligands, is responsible for 77% of the absorbance at 810–820 nm, whereas the contribution of heme a and heme a<sub>3</sub>/Cu<sub>B</sub> is 18 and 5%, respectively.<sup>16</sup> Due to the domination of the strong absorption of Cu<sub>A</sub> in this region, weak underlying lines are masked in the absorption spectrum of cytochrome c oxidase.<sup>17</sup> A distance of 33.5 nm between the minimal and maximal peak positions in the spectra (Table 1) is too long to be explained by measurement error (e.g., FWHM of irradiating light 10 or 14 nm). Quite probably, different lines in absorption spectra of intermediates of cytochrome c oxidase appear in the action spectra. This suggestion, however, requires further experimental proof.

The maximum in spectra A–E in Figure 3 has peak positions from 750.7 to 772.3 nm (Table 1). In four spectra, this peak is at 761.1–772.3 nm, which could be one line in absorption spectra. An appearance of this maximum with peak position at 750.7 nm in spectrum E could probably mirror another line in absorption spectra. The origin of lines in 750–770 nm as absorption spectra of cytochrome c oxidase is not fully understood, but the mitochondria account for about 50% of the liver absorption coefficient in this region.<sup>18</sup>

A study of the near-IR absorption spectra of membrane-bound cytochrome c oxidase at low temperature shows that there are overlapping traces covering the full wavelength range of 680–870 nm. Flash photolysis causes the formation of a mixed valence compound with a peak at 740–750 nm, which could belong to invisible copper (Cu<sub>B</sub>).<sup>19</sup> A band at ~785 nm is present in fully reduced unliganded five coordinated ferrous heme a<sub>2</sub><sup>+</sup>.<sup>20</sup> The addition of carbon monoxide to the reduced enzyme causes a blue shift from 785 to 760 nm in the difference spectrum, and the photodissociation of CO results in a reversion of the band from 760 to 784 nm.<sup>17</sup>

The far-red maximum in the action spectra (Fig. 3) has peak positions from 667.5 to 684.5 nm. These peak positions can be divided into two groups: 667.5, 671.5, and 668.0 nm in one group, and 684.5 and 683.7 nm in another (Table 1). In the wavelength range at 670–680 nm, there are no absorption bands of cytochrome c oxidase intermediates recorded so far. A small absorption band belonging to an intermediate (compound A) has been recorded at ~660 nm.<sup>16</sup> The appearance of the 655-nm absorption band suggests that Cu<sub>B</sub> is oxidized and participating in a spin-coupled state.<sup>21</sup> It is suggested that the 655-nm feature may arise from a charge transfer band of ferric high-spin heme a<sub>3</sub>, which is modulated by the redox state of

Cu<sub>B</sub>. The 655-nm band disappears as the binuclear center is reduced.<sup>22</sup>

The red maximum in the action spectra (Fig. 3) has peak positions from 613.5 to 623.5 nm (Table 1). Quite probably, this is one line in the absorption spectra of cytochrome c oxidase and/or its intermediates. It has been known for a long time that reduced cytochrome c oxidase has a peak at 605 nm, and this peak has been recorded both in mitochondria and whole cell.<sup>23</sup> For membrane-bound cytochrome c oxidase, this peak can be red-shifted ~10 nm as compared to solubilized enzyme.<sup>24</sup> Some isospectral peroxy intermediates have a peak at ~607 nm in their absorption spectra.<sup>25</sup> The absorption of this region is arising 75% due to low-spin heme a<sub>3</sub>, and 25% by high-spin heme a<sub>3</sub>. However, a definite contribution of Cu<sub>A</sub> at ~615 nm has been suggested as well.<sup>26</sup>

It should be noted that, in an early action spectrum, a peak at 606 nm appeared together with a peak at 632.8 nm (Fig. 4A, Table 2). These first two spectra for stimulation of DNA and RNA synthesis rate were recorded from 570 to 650 nm using filament lamps with a power of 20 and 90 W, and interference

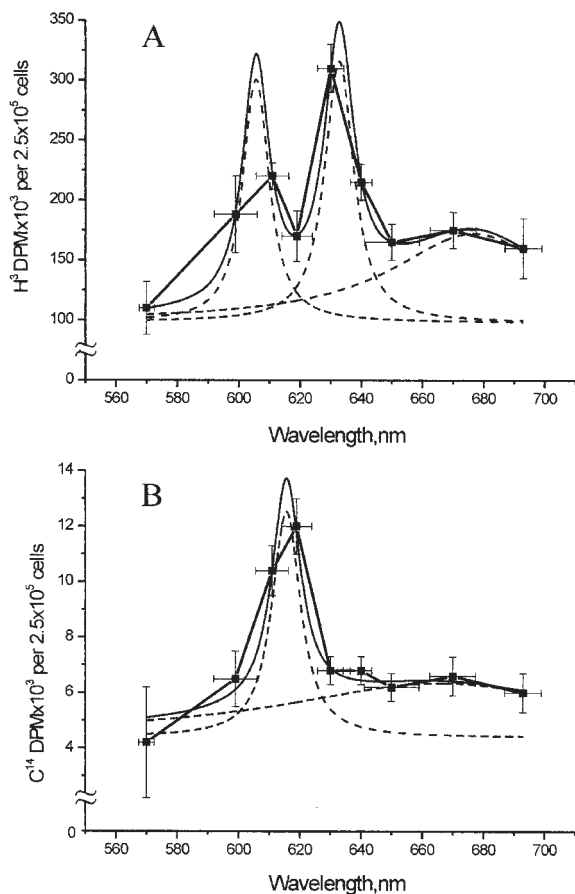


**FIG. 4.** Action spectra in the region of 570–650 nm for the stimulation of DNA (A) and RNA (B) synthesis rate in log-phase cultures at  $D = 80 \text{ J/m}^2$  under conditions where irradiation times were not kept constant. Experimental curves (—■—; <sup>3</sup>), curve fittings (—), and Lorentzian fittings (---) are shown.

**TABLE 2.** PARAMETERS OF THE BANDS IN ACTION SPECTRA IN FIGURE 4 DETERMINED BY DECONVOLUTION OF SPECTRA WITH LORENTZIAN FITTING

Stimulation of DNA synthesis rate, (Fig. 4A) $R^2 = 1$		Stimulation of RNA synthesis rate, (Fig. 4B) $R^2 = 0.97$	
Peak position, nm	FWHM, nm	Peak position, nm	FWHM, nm
606.0	9.5	616.0	10.6
632.8	10.6	—	—
677.0	65.7	666.1	127.1

$R^2$ , mean-square deviation; FWHM, full width of the band at half maximal height.

filters.<sup>3</sup> With that setup, we were not able to keep equal intensity of light at all wavelengths. This means that, for a constant dose, one was forced to use various irradiation times. In our case, the intensity was 1.5 and 0.3 W/m<sup>2</sup>, and the dose of 80 J/m<sup>2</sup> was reached by irradiating the cells from 2 sec to 4.5 min. This was not a correct measurement of an action spectrum, but at that time this first experiment showed several important features of the biostimulation phenomenon. First, not only He-Ne laser light at 632.8 nm causes “biostimulation,” a similar result was achieved using noncoherent light of the same wavelength. Recall that, in year 1982, the medical laser community believed that He-Ne laser radiation had magical beneficial properties. Secondly, after improving the equipment and comparing new action spectra (Fig. 3A–D) to the first spectra presented in Figure 4A,B, we understood that there should be a dependence on light intensity in the far-red region of 650–680 nm. Speaking in photobiological terms, the reciprocity rule does not hold. According to the reciprocity (or Bunsen-Roscoe) rule, a photochemical reaction is directly proportional to the total energy dose, irrespective of the time over which this dose is delivered.<sup>2</sup> However, the reasons why in one spectrum (Fig. 4A) two red bands appeared, are still obscure. One can only suppose that this is due to irradiation parameters, intensity, and irradiation time. Solving this question requires new experiments.

Our finding of this absence of reciprocity led us to perform a special experiment where the dose was kept constant but the irradiation time and intensity were varied. These data are presented here to draw attention to the threshold-type behavior of intensity-dependence, which is still not understood and often not taken into account in experiments. It appeared that the red maximum in the action spectra is sensitive to light intensity (Fig. 5) and that there exists a certain threshold to receive a stimulation effect (in our case at 4–5 W/m<sup>2</sup>). The maximum effect occurred near 8 W/m<sup>2</sup> (irradiation time 10–12 sec). The existence of the intensity threshold is especially important from practical point of view (both in the laboratory and clinic) in deciding on the irradiation parameters. A similar type of curve was recorded at 454 nm for *E. coli*.<sup>10</sup> Later, the invalidity of the reciprocity rule was shown for light with  $\lambda = 632.8 \text{ nm}$  when irradiating human fibroblasts<sup>27</sup> and *E. coli*.<sup>28</sup> It is clear that the same type of measurements are needed for all bands in action spectra.

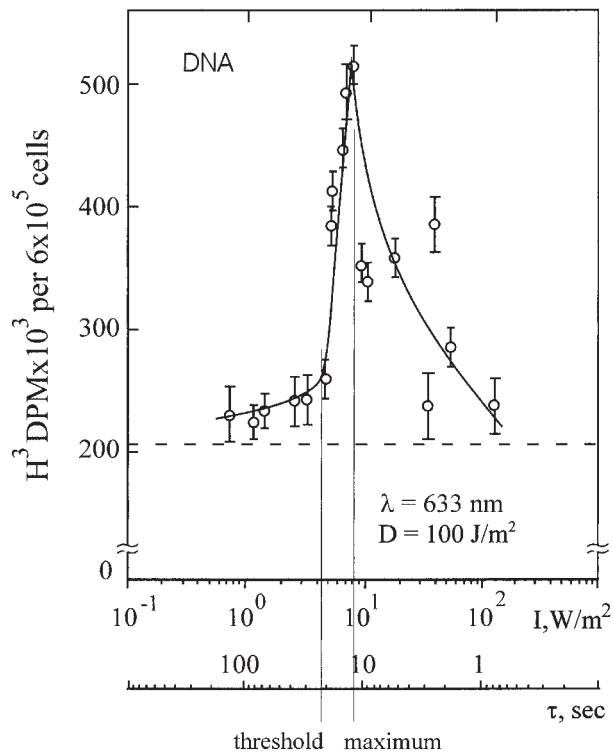


**FIG. 5.** Dependence of stimulation of DNA synthesis rate on light intensity or irradiation time at a constant dose measured 1.5 h after irradiation of log-phase cells with a continuous-wave dye laser pumped by an argon laser ( $\lambda = 633$  nm,  $I_{\max} = 80$  W/m<sup>2</sup>).<sup>4</sup> Dashed line shows the control level.

In the wavelength range used in our experiments and important for phototherapy (600–860 nm), there are four “active” regions, but the peak positions are not exactly the same for all action spectra. The red band has peak position at 613.5–623.5 nm (in one spectrum, at 606 nm); the far-red band has peak position at 667.5–683.7 nm, and two near IR bands in the range of 750.7–772.3 nm and 812.5–846.0 nm. The nature of the cytochrome c oxidase intermediates, whose absorption spectrum is mirrored in these action spectra, remains to be investigated.

### ACKNOWLEDGMENTS

L.V. Pyatibrat and A.F. Kornushkin are thanked for technical help and Dr. N. Afanasyeva for useful discussions.

### REFERENCES

- Smith, K.C. (2005). Laser (and LED) therapy is phototherapy. *Photomed. Laser Surg.* 23:78–80.
- Hartmann, K.M. (1983). Action spectroscopy, in: W. Hoppe, W. Lohmann, H. Marke, et al. (eds.). Springer: Heidelberg, *The Biophysics*. pp. 115–144.
- Karu, T.I., Kalendo, G.S., Letokhov, V.S., et al. (1982). Biostimulation of HeLa cells by low intensity visible light. *Nuovo Cimento D* 1:828–840.
- Karu, T.I., Kalendo, G.S., Letokhov, V.S., et al. (1984). Biostimulation of HeLa cells by low-intensity visible light. II. Stimulation of DNA and RNA synthesis in a wide spectral range. *Nuovo Cimento D* 3:308–318.
- Karu, T.I., Kalendo, G.S., Letokhov, V.S., et al. (1984). Biostimulation of HeLa cells by low intensity visible light. III. Stimulation of nucleic acid synthesis in plateau phase cells. *Nuovo Cimento D* 3:319–325.
- Karu T.I. (1987). Photobiological fundamentals of low-power laser therapy. *IEEE J. Quantum Electronics QE-23*: 1703–1717.
- Karu, T.I., Letokhov, V.S., and Lobko V.V. (1985). Biostimulation of HeLa cells by low-intensity visible light. IV. Dichromatic irradiation. *Nuovo Cimento D* 5:483–496.
- Karu T.I. (1988). Molecular mechanism of the therapeutic effect of low-intensity laser radiation. *Lasers Life Sci.* 2:53–74.
- Karu T.I. (1999). Primary and secondary mechanisms of action of visible-to-near IR radiation on cells. *J. Photochem. Photobiol. B Biol.* 49:1–17.
- Tiphlova, O. and Karu, T. (1991). Action of low-intensity laser radiation on *Escherichia coli*. *CRC Crit. Rev. Biomed. Eng.* 18: 387–412.
- Wong-Riley, M.T.T., Liang, H.L., Eells, J.T., et al. (2005). Photobiomodulation directly benefits primary neurons functionally inactivated by toxins: role of cytochrome c oxidase. *J. Biol. Chem.* 280:4761–4771.
- Karu, T.I., Pyatibrat, L.V., Kalendo, G.S., et al. (1996). Effects of monochromatic low-intensity light and laser irradiation on adhesion of HeLa cells *in vitro*. *Lasers Surg. Med.*, 18, 171–177.
- Karu, T.I., Pyatibrat, L.V., and Kalendo, G.S. (1987). Biostimulation of HeLa cells by low-intensity visible light. V. Stimulation of cell proliferation *in vitro* by He-Ne laser radiation. *Nuovo Cimento D* 9:1485–1494.
- Karu, T. (1998). *The Science of Low Power Laser Therapy*. London: Gordon and Breach, pp. 46–47.
- Griffiths, D.E., and Wharton, D.C. (1961). Studies of the electron transport system. XXXV. Purification and properties of cytochrome oxidase. *J. Biol. Chem.* 236:1850–1856.
- Szundi, I., Liao, G.-L., and Einarsdottir, O. (2001). Near-infrared time-resolved optical absorption studies of the reaction of fully reduced cytochrome c oxidase with dioxygen. *Biochemistry* 40: 2332–2339.
- Rich, P.R., Moody, A.J., and Ingledew, W.J. (1992). Detection of near infra-red absorption band of ferrohaem a<sub>3</sub> in cytochrome c oxidase. *FEBS Lett.* 305:171–173.
- Beauvoit, B., Ketai, T., and Chance, B. (1994). Contribution of the mitochondrial compartment to the optical properties of the rat level: a theoretical and practical approach. *Biophys. J.* 67 2501–2510.
- Chance, B., and Leigh, J.S. (1977). Oxygen intermediates and mixed valence states of cytochrome c oxidase: infrared absorption difference spectra of compounds A, B, and C of cytochrome oxidase and oxygen. *Proc. Natl. Acad. Sci. USA* 74:4777–4780.
- Einarsdottir, O., Georgiadis, K.E., and Dawes, T.D. (1992). Evidence for a band III analogue in the near-infrared absorption spectra of cytochrome c oxidase. *Biochem. Biophys. Res. Commun.* 184:1035–1041.
- Shaw, R.W., Hansen, R.E., and Beinert, H. (1979). The oxygen reactions of reduced cytochrome c oxidase. Position of a form with an unusual EPR signal in the sequence of early intermediates. *Biochem. Biophys. Acta* 548:386–396.
- Mitchell, R., Mitchell, P., and Rich, P. (1991). The assignment of 655-nm spectral band of cytochrome c oxidase. *FEBS Lett.* 280: 321–324.
- Chance, B., and Hess, B. (1959). Spectroscopic evidence of metabolic control. *Science* 129:700–708.

24. Clore, M. (1980). Characterization of the intermediates in the reaction of membrane-bound mixed-valence-state cytochrome oxidase with oxygen at low temperatures by optical spectroscopy in the visible region. *Biochem. J.* 187:617–622.
25. Szundi, I., Cappuccio, J., and Einarsdóttir, O. (2004). Amplitude analysis of single-wavelength time-dependent absorbing data does not support the conventional sequential mechanism for the reduction of dioxygen to water catalyzed by bovine heart cytochrome c oxidase. *Biochemistry* 43:15746–15758.
26. Brunori, M., Antonini, E., and Wilson, M.T. (1981). Cytochrome c oxidase: an overview of recent work, in: *Metal Ions in Biological Systems*. Vol. 13. H. Siegel (ed.). New York: Marcel Dekker, pp. 187–228.
27. van Breugel, H.H.F.I., and Dop Bär, P.R. (1992). Power density and exposure time of He-Ne laser irradiation are more important than total energy dose in photobiomodulation of human fibroblasts *in vitro*. *Lasers Surg. Med.* 12:528–537.
28. Karu, T., Tiphlova, O., Esenaliev, R., et al. (1994). Two different mechanisms of low-intensity laser photobiological effects on *Escherichia coli*. *J. Photochem. Photobiol. B Biol.* 24:155–161.

Address reprint requests to:

Dr. T.I. Karu  
Institute of Laser and Information Technologies  
Russian Academy of Sciences  
142190 Troitsk, Moscow Region  
Russian Federation

E-mail: tkaru@isan.troitsk.ru